

---

# Using Reinforcement Learning to Train Large Language Models to Explain Human Decisions

---

**Jian-Qiao Zhu\***

Department of Computer Science  
Princeton University

**Hanbo Xie\***

School of Psychology  
Georgia Institute of Technology

**Dilip Arumugam**

Department of Computer Science  
Princeton University

**Robert C. Wilson\*\***

School of Psychology  
Georgia Institute of Technology

**Thomas L. Griffiths\*\***

Departments of Psychology and Computer Science  
Princeton University

## Abstract

A central goal of cognitive modeling is to develop models that not only predict human behavior but also provide insight into the underlying cognitive mechanisms. While neural network models trained on large-scale behavioral data often achieve strong predictive performance, they typically fall short in offering interpretable explanations of the cognitive processes they capture. In this work, we explore the potential of pretrained large language models (LLMs) to serve as dual-purpose cognitive models—capable of both accurate prediction and interpretable explanation in natural language. Specifically, we employ reinforcement learning with outcome-based rewards to guide LLMs toward generating explicit reasoning traces for explaining human risky choices. Our findings demonstrate that this approach produces high-quality explanations alongside strong quantitative predictions of human decisions.

## 1 Introduction

Computational models of cognition have driven immense progress in understanding the mental processes underlying learning, thinking, problem solving, and decision making [9, 5, 15, 25, 30]. Recent advances—particularly those leveraging neural networks to predict human behavior—have introduced increasingly sophisticated model architectures and training methods [26, 42, 17, 1]. While these models have demonstrated improved predictive accuracy, they often lack interpretability, offering limited insight into the underlying cognitive mechanisms. A recent example is the Centaur model, which applies customized supervised fine-tuning (SFT) to pretrained LLMs and achieves impressive performance in predicting human behavior, surpassing domain-specific cognitive models from the literature [2]. However, despite their predictive successes, such models offer limited explanatory power; a deeper theoretical understanding of human cognition requires more than a simple match in behavior [11].

To start addressing this dilemma, we propose that LLMs capable of generating reasoning or thinking tokens offer a promising opportunity for developing cognitive models that not only *predict* but also

---

\*Equal contribution, \*\*Equal advising. Correspondence to: Jian-Qiao Zhu <jz5204@princeton.edu>

*explain* human behavior. The key idea is to treat the chain-of-thought (CoT) generated by these models prior to their final responses as a verbalized account of underlying cognitive mechanisms, expressed in natural language. In other words, while LLMs learn to generate CoT reasoning that improves prediction of human behavior, cognitive scientists can examine these CoTs to assess whether they provide meaningful and interpretable explanations of the observed data.

In this work, we put these ideas to the test in the domain of human risky choice. That is, how people choose between risky and/or safe options. To encourage LLMs to generate both CoTs and predictions about human risky choices, we post-train a backbone LLM using reinforcement learning (RL) with outcome-based rewards [20, 32, 39, 23], where human choice proportions served as the ground truth for evaluation. To contextualize the RL approach, we also evaluated various SFT post-training methods, including Centaur-style SFT [2].

Our findings show that RL post-training can elicit sensible CoT reasoning traces from LLMs while achieving predictive accuracy comparable to that of SFT-based methods. Moreover, the generated CoTs are responsive to the structure of the training data: when human behavioral data are replaced with synthetic data generated by an expected-value maximization model, the CoTs adapt accordingly to reflect the structure of the synthetic dataset. We also find that the quality of the CoTs depends on the strength of the backbone LLM and thus using a weaker model results in noticeable degradation of reasoning quality.

## 2 Related Work

**Leveraging LLMs to model human cognition.** In recent years, there has been widespread enthusiasm about the potential of LLMs to advance cognitive modeling and provide new theoretical understanding about the mind. A growing body of work has sparked scholarly debate around the use of LLMs for modeling human cognitive processes [11, 15, 3]. The main advantage of using LLMs to predict human behavior is that LLMs can process similar stimuli to people; in other words, LLMs can process a broader range of stimuli (often described in natural language) than previous neural network models which typically operate in a more abstract representation of cognitive tasks.

Consider the risky choice problem illustrated in Figure 1 as an example. Traditional cognitive models and neural-network-based models typically operate on structured quantitative task features such as  $\{1, \$27\}$  (i.e., probability and value) for option A and  $\{0.9, \$25; 0.1, \$92\}$  for option B [26]. These models define functions that map from such numerical inputs to human risky choices. In contrast, LLM-based cognitive models operate over a different representation of the task: they take natural language descriptions as input and predict human responses directly [43, 2, 3]. Recent work has shown that SFT of LLMs can improve predictive accuracy on human behavioral data [2].

**Automated discovery of cognitive models using LLMs.** Another closely-related line of research involves using LLMs to automatically search over the space of cognitive models, enabling the automated discovery of interpretable theories [6, 29]. In this approach, LLMs are prompted to generate symbolic programs (i.e., Python code), which are then executed and fitted to human or animal data. Because the discovered models are expressed as code, they are inherently interpretable—helping to address the aforementioned dilemma in cognitive modeling. Leveraging the coding capabilities of LLMs has shown promise in identifying heuristic decision-making models [29] and strategies in multi-armed bandit tasks [6]. However, these approaches typically do not involve further fine-tuning of the LLM during the search process, instead relying heavily on the model’s in-context learning [4] ability for effective model discovery.

## 3 Method

To evaluate whether post-training LLMs can produce useful cognitive models, we compare three distinct post-training strategies for LLMs: (i) SFT, (ii) a variant of SFT specifically designed for adapting LLMs to cognitive tasks, as used in the Centaur model [2], and (iii) RL based on Group Relative Policy Optimization (GRPO) [32, 23]. Each method was applied to fine-tune identical low-rank adaptation (LoRA) modules on the largest available human risky-choice dataset, `choices13k`, originally collected by [26].

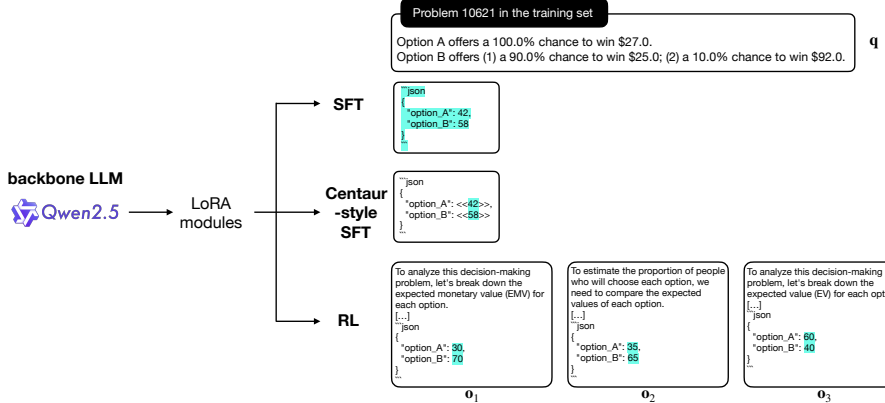


Figure 1: Overview of three post-training strategies for building cognitive models of human risky choice using Qwen-2.5-7B-Instruct. The backbone LLM was first adapted using low-rank adaptation (LoRA) [16], followed by post-training via three strategies: supervised fine-tuning (SFT), Centaur-style SFT [2], and reinforcement learning from outcome-based rewards [23, 32]. In the illustrated example, the LLM is prompted to predict human choice behavior. SFT and Centaur-style models are trained directly on human data represented in JSON format. In contrast, the RL model generates candidate completions that include CoT reasoning and final predictions in JSON format, with each completion evaluated based on its predictions. Tokens or predictions relevant to each training method are highlighted in light blue.

The backbone LLM used throughout is Qwen-2.5-7B-Instruct [38]. All models were fine-tuned using the same LoRA configuration [16], with both the rank and alpha parameters set to 32. LoRA modules were applied to all linear layers of the backbone model and included a dropout probability of 0.05. This setup results in approximately 80.74M trainable parameters, comprising only 1.05% of the total parameters in the 7B model.

To ensure consistency and control across training and evaluation, we randomly partitioned the choices13k dataset into training and test sets using a 90/10 split, resulting in 13,102 choice problems for training and 1,462 for testing. The partition was performed at the level of unique problem identifiers, such that repeated measures of the same problem, if present, were assigned entirely to either the training or the test set. This partition was held fixed for all post-training, including SFT, Centaur-style SFT, and RL, as well as evaluation procedures.

**SFT and Centaur-style SFT training details.** We begin with the standard SFT approach to adapt a pretrained LLM to the target domain of human risky choice behavior (see Figure 1 SFT). To enhance the Qwen model’s ability to predict human decisions, we converted the original choices13k dataset into a text format. Specifically, we represented human choice data in JSON, rounding the observed choice percentages for each option to the nearest integer between 0 and 100. For example, if empirical data show that 71.11% of participants selected Option B, this was reformatted as JSON: `{"option_A": 29, "option_B": 71}`. See Appendix A.1 for detailed prompts.

We fine-tuned the Qwen model using SFT for a total of 6 epochs on the training set, with a fixed learning rate of  $10^{-5}$ , gradient accumulation steps of 8, and the AdamW optimizer [24]. In our setup, SFT corresponds to the standard autoregressive next-token prediction paradigm.

In parallel, we implemented a variant used to train the Centaur model, which selectively masks out all tokens except those corresponding to human data [2]. This method has been shown to effectively adapt pretrained LLMs for explaining a wide range of human cognitive tasks [2]. Unlike standard SFT, Centaur-style SFT places human data (i.e., choice proportions) within special brackets (“`<<`” and “`>>`”), and only tokens enclosed within these brackets contribute to the loss during training (see Figure 1). In our implementation, Centaur-style SFT was applied at the problem level rather than the individual participant level, such that the model predicts aggregated human responses for each risky-choice problem.

**RL training details.** We also fine-tuned the Qwen model using the GRPO algorithm [32]. At each training step, the model generates 12 candidate completions (i.e.,  $\mathbf{o}_1, \mathbf{o}_2, \dots, \mathbf{o}_G$ ) for the same risky-

choice problem (i.e.,  $\mathbf{q}$ ), with each completion capped at a maximum length of 1,024 tokens. The GRPO algorithm evaluates each candidate based on the model-predicted choice probabilities for the two options (see Figure 1 RL). Specifically, we implemented a outcome-based reward function that uses human data as ground truth. The reward is defined as one minus the absolute difference between the model’s predicted probability for option B and the empirical proportion of human participants who chose that option:

$$R(\mathbf{q}, \mathbf{o}) = \begin{cases} 1 - |\mathbf{o}^B - \mathbf{p}^B| & \text{if } \mathbf{o} \text{ is coherent} \\ 0 & \text{otherwise} \end{cases} \quad (1)$$

Here,  $\mathbf{q}$  denotes the risky-choice problem,  $\mathbf{o}$  is the model response,  $\mathbf{o}^B$  is the model-predicted probability for option B, and  $\mathbf{p}^B$  is the proportion of human participants who selected option B. To be eligible for a reward, model-predicted probabilities for both option A and B must satisfy coherence constraints:  $0 \leq \mathbf{o}^A \leq 1$ ,  $0 \leq \mathbf{o}^B \leq 1$ , and  $\mathbf{o}^A + \mathbf{o}^B = 1$ . The maximum achievable outcome reward is 1, which occurs when  $\mathbf{o}^B = \mathbf{p}^B$ .

In addition, we incorporated a format reward to encourage structurally well-formed completions. This reward depends on the number and position of JSON-formatted outputs in the model response. If the model generates exactly one JSON output, the format reward increases by 0.25. Furthermore, if the first JSON output appears after the 500th character—encouraging reasoning tokens to precede the prediction—the format reward increases by an additional 0.25. The maximum possible format reward is therefore 0.5.

The RL training was conducted for a total of 3 epochs, with a learning rate of  $3 \times 10^{-6}$  and a cosine learning rate scheduler. Moreover, we omitted the reward normalization by standard deviation as suggested by the GRPO Done Right algorithm [23]. As a result, the advantage function was defined as the reward of each candidate completion minus the average reward within the group.

$$A_i = R(\mathbf{q}, \mathbf{o}_i) - \text{mean}(\{R(\mathbf{q}, \mathbf{o}_1), \dots, R(\mathbf{q}, \mathbf{o}_G)\}) \quad (2)$$

where  $G = 12$  is the group size. We revisit the implications of this design choice, along with other unsuccessful attempts, in the Discussion section.

With the advantage function defined, we train the backbone LLM using the GRPO Done Right algorithm with the following objective function:

$$\begin{aligned} \mathcal{L}(\pi_\theta) = & \mathbb{E}_{\mathbf{q} \sim Q, \{\mathbf{o}_i\}_{i=1}^G \sim \pi_{\theta_{\text{old}}}(\cdot | \mathbf{q})} \\ & \frac{1}{G} \sum_{i=1}^G \sum_{t=1}^{|\mathbf{o}_i|} \left\{ \min \left[ \frac{\pi_\theta(o_{i,t} | \mathbf{q}, \mathbf{o}_{i,<t})}{\pi_{\theta_{\text{old}}}(o_{i,t} | \mathbf{q}, \mathbf{o}_{i,<t})} A_i, \text{clip}\left(\frac{\pi_\theta(o_{i,t} | \mathbf{q}, \mathbf{o}_{i,<t})}{\pi_{\theta_{\text{old}}}(o_{i,t} | \mathbf{q}, \mathbf{o}_{i,<t})}, 1 - \epsilon_{\text{low}}, 1 + \epsilon_{\text{high}}\right) A_i \right] \right\} \end{aligned} \quad (3)$$

where  $\mathbf{q}$  denotes a risky-choice problem sampled from the training set  $Q$ , and  $|\mathbf{o}_i|$  is the number of tokens in the  $i$ -th model completion  $\mathbf{o}_i$ , generated by the LLM under the old policy  $\pi_{\theta_{\text{old}}}$ . Moreover,  $t$  denotes the position of a token within the sequence of a model-generated completion and  $\theta$  represents the parameters of LLM. The inner summation iterates over all tokens in the sampled completion. This objective follows the clipped surrogate loss formulation from the proximal policy optimization (PPO) algorithm [31], modified to operate at the token level within each sampled trajectory. The clipped values lie within the range of [0.8, 1.28], where  $\epsilon_{\text{low}} = 0.2$  and  $\epsilon_{\text{high}} = 0.28$ , as set in our experiment. This asymmetric clipping follows the recommendation in [39], which suggests that slightly increasing  $\epsilon_{\text{high}}$  can enhance exploration in RL. GRPO also incorporates a KL divergence penalty term in its objective function to prevent the updated policy from deviating too far from the backbone LLM. This penalty takes the form  $\beta D_{KL}(\pi_\theta \| \pi_{\text{reference}})$ , where  $\beta$  is set to  $10^{-4}$ .

**Key distinctions between RL and Centaur-style SFT.** While both Centaur-style SFT and RL focus exclusively on tokens relevant to choice probabilities (see Figure 1, highlighted text), there are important distinctions between these two post-training methods. Centaur-style SFT operates within the standard next-token prediction framework and thus relies on the tokenized representation of numerical outputs. In contrast, RL assigns outcome rewards based on the predicted numerical values themselves, rather than their tokenized forms. These rewards are then used to weight policy updates during training. This reward-weighted policy optimization has been argued to support improved generalization in downstream tasks [7, 37].

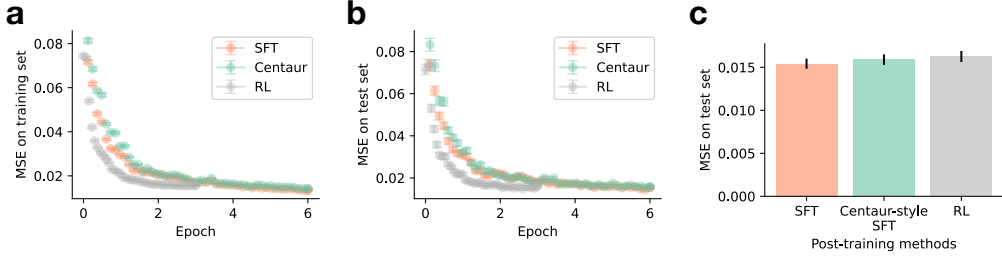


Figure 2: Learning curves on the (a) training and (b) test sets. Backbone LLM is Qwen-2.5-7B-Instruct. The horizontal axes indicate training epochs, while the vertical axes represent mean squared error (MSE) evaluated on the corresponding dataset. The three post-training strategies compared are supervised fine-tuning (SFT, red), Centaur-style SFT (green), and reinforcement learning (RL, grey). The lowest MSEs on the training set occur at epochs 5.98 (SFT), 5.74 (Centaur-style SFT), and 2.75 (RL), while the lowest MSEs on the test set occur at epochs 5.86 (SFT), 5.86 (Centaur-style SFT), and 2.60 (RL). (c) MSE on the test set at the final checkpoint of each post-training method. Error bars represent  $\pm 1$  standard error across risky-choice problems.

## 4 Results

Having introduced the three post-training strategies, we now evaluate the effectiveness of the fine-tuned models from each method as cognitive models of human risky choice. To ensure comparability, all fine-tuned models were evaluated using identical sampling parameters, implemented with vLLM [19]: temperature = 0.7, top-p = 0.95, and top-k = 50. The maximum number of generated tokens was adjusted according to model type. Since the RL models were trained to generate intermediate reasoning before producing a final choice prediction, they were allowed up to 1,024 tokens to accommodate more elaborate completions. In contrast, the SFT and Centaur-style models were restricted to 30 tokens, as they were trained to produce choice predictions directly without intermediate reasoning steps. We evaluated model inferences at all checkpoints across the three post-training methods, for both the training and test set problems.

**Learning curves.** All three post-training methods led to gradual improvements in model predictions, as indicated by decreasing MSE on both the training and test sets (see Figure 2). However, the error trajectories differ notably across methods. RL achieves a faster reduction in prediction error compared to SFT and Centaur-style SFT when measured by the number of training examples processed. It is important to note, however, that RL generates significantly more completions per training example and incurs substantially higher computational costs, whereas SFT and Centaur-style SFT are trained directly on the human data without generating additional completions.

Ultimately, all three post-training methods yield fine-tuned models with comparable performance in predicting human choices. At the final checkpoint, the MSE on test set is  $M = .0144$  ( $SE = .0006$ ) for SFT,  $M = .0155$  ( $SE = .0006$ ) for Centaur-style SFT,  $M = .0148$  ( $SE = .0006$ ) for RL. Statistical tests reveal no significant differences among the models: SFT vs. Centaur-style SFT ( $t(2923) = -1.31, p = 0.19$ ), SFT vs. RL ( $t(2921) = -0.58, p = 0.56$ ), and RL vs. Centaur-style SFT ( $t(2920) = 0.78, p = 0.43$ ). For reference, the best-performing neural network model reported in [26], the Mixture of Theories model, achieved an MSE of .0113, while the neurally augmented prospect theory model achieved an MSE of .0204 (both models use problem features as input rather than text).

Moreover, we observe stable improvements in the RL learning curves for both the correctness reward and the format reward (see Figure 3). The format reward is learned rapidly, with the ceiling value of 0.5 reached within the first few training steps. The completion length of the RL model initially increases during the first training epoch and subsequently stabilizes between 500 and 650 tokens.

**Analyzing Chains-of-Thought.** Unlike the SFT and Centaur-style models, RL models are capable of explicitly generating reasoning tokens prior to making final predictions. We analyze these reasoning chains with three key objectives: (i) to characterize the nature of the reasoning processes across different risky-choice problems and training stages; (ii) to assess whether the reasoning chains exhibit

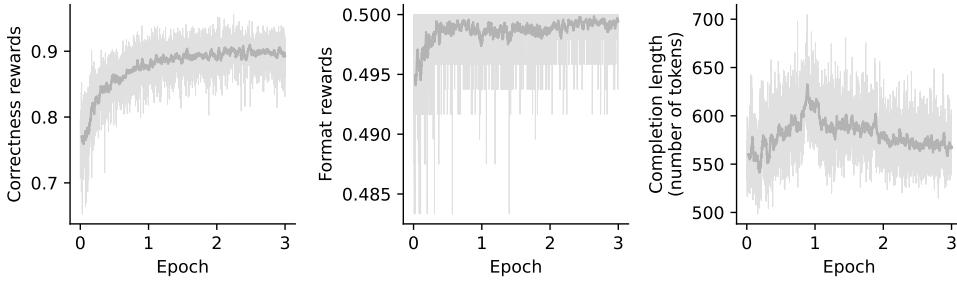


Figure 3: Learning curves for the RL model. Backbone LLM is Qwen-2.5-7B-Instruct. (*Left*) Correctness reward, defined as one minus the absolute difference between model predictions and human choice proportions. (*Middle*) Format reward, based on the structure and position of the model’s JSON output. (*Right*) Completion length, measured by the number of generated tokens.

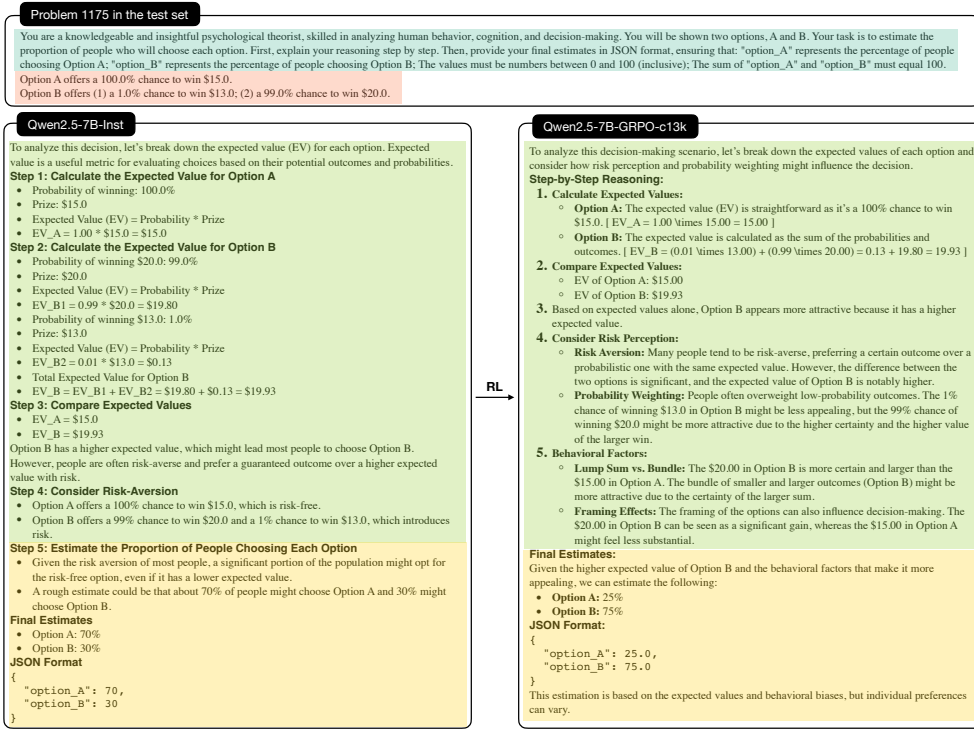


Figure 4: Comparison of CoT reasoning and model predictions before (left panel) and after (right panel) RL training. Human data indicate that approximately 71% of participants selected Option B in this problem. Model completions are reformatted using Markdown for enhanced readability.

causal influence on the model’s predictions; and (iii) to examine the implications of these reasoning traces for developing cognitive models of human risky choice.

As illustrated in Figure 4, RL training alters both the CoT reasoning and final predictions of the LLM for the same problem in the held-out test set. We observe that certain thoughts are preserved: for example, the calculation and comparison of expected values for both options, as well as considerations of human risk preferences. In addition, RL appears to amplify certain types of thoughts in the CoT, such as references to psychological factors and cognitive biases.

We next aim to characterize the CoT reasoning learned by the RL model in order to identify effective cognitive processes that contribute to accurately predicting human risky choices. Note that the CoT generated by the RL model is typically itemized, often presented as a sequence of clearly delineated steps or sections. Leveraging this structure, we segmented each CoT into smaller units—referred to as

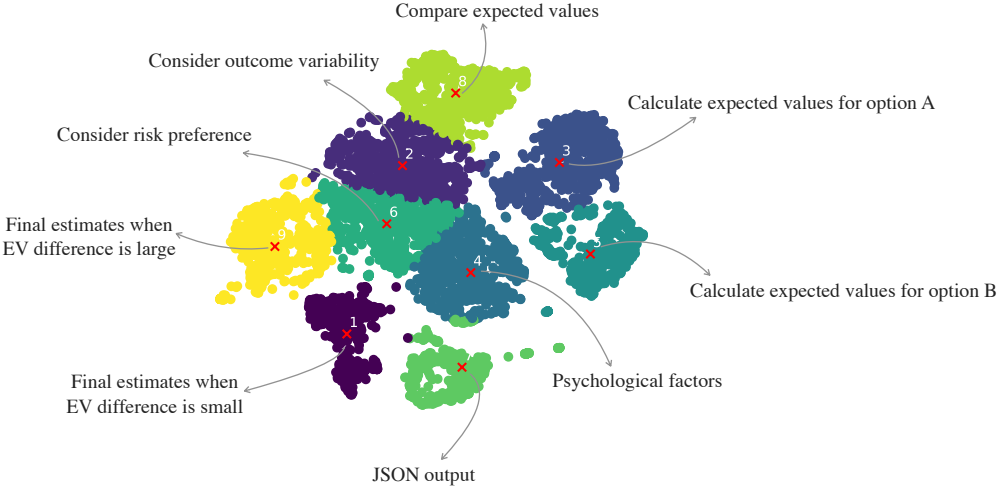


Figure 5: Visualization of CoT reasoning generated by RL models. Each reasoning segment (“thought”) is embedded using the all-MiniLM-L6-v2 model from SBERT [28], followed by dimensionality reduction to two dimensions using t-SNE [36]. In the resulting 2D space, we identified nine clusters using the k-means algorithm. Each cluster is labeled with a summary of its centroid thought to provide an interpretable overview of common reasoning patterns.

thoughts—using a regular expression-based parser. For example, the CoT shown in Figure 5 (right) is divided into five distinct thoughts, corresponding to its five itemized sections.

Each segmented thought was embedded using the all-MiniLM-L6-v2 model from SBERT [28], and subsequently projected into two dimensions using t-SNE for visualization [36]. In this 2D embedding space, we identified nine clusters using the k-means algorithm. To enhance interpretability, each cluster was labeled with a summary of its centroid thought, providing an overview of common reasoning patterns.

As shown in Figure 5, the CoT generated by the RL model can be broadly categorized into five types of reasoning strategies that contribute to improved prediction of human risky choices: (i) computing the expected values of both options accurately, (ii) conducting a coarse comparison based on these expected values, (iii) considering psychological influences such as behavioral biases, (iv) incorporating human risk preferences and the variability of outcomes, and (v) producing a final prediction based on some or all of the above factors, conditional on the magnitude of the expected value difference.

Moreover, we conducted several supplementary analyses of CoT reasoning, including small-scale human evaluations (Appendix C.1), large-scale LLM-as-a-judge assessments (Appendix C.2), and CoT swapping between the backbone and RL models (Appendix C.3). Taken together, these analyses suggest that RL post-training improves the quality of CoT reasoning, which in turn contributes to enhanced prediction accuracy of human behavior.

**Cognitive mechanisms identified in CoT.** We examined the cognitive mechanisms reflected in the RL model’s CoT reasoning. To assist with this analysis, we used GPT-4.1<sup>2</sup> to summarize the CoT outputs generated by the RL model (see Appendix B for detailed prompts). The evolution of the top eight cognitive mechanisms over training epochs is shown in Figure 6a. Among these, expected value computation and risk aversion emerged as the two most frequently used mechanisms, each accounting for approximately 29% to 36% of thoughts across risky-choice problems.

We observed notable representations of loss aversion—the tendency for individuals to prefer avoiding losses over acquiring equivalent gains [35]—and the certainty effect, where individuals disproportionately favor certain outcomes over those that are merely probable [8]. Finally, the RL model occasionally considers the possibility that some individuals may exhibit risk-seeking behavior or be

<sup>2</sup><https://openai.com/index/gpt-4-1/>

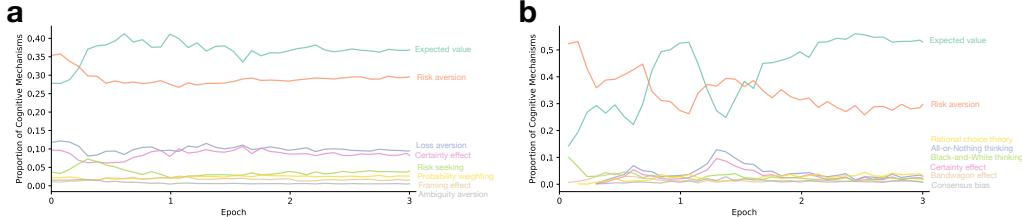


Figure 6: Proportions of cognitive mechanisms identified in the RL models’ thoughts across training epochs. Backbone LLM is Qwen-2.5-7B-Instruct. The top eight most frequently used mechanisms are displayed. **(a)** Training data are human risky choices. **(b)** Training data are synthetic choices generated by an expected-value maximization model.

influenced by other cognitive biases, such as probability weighting [27, 18], framing effects [34], and ambiguity aversion [10]. The full list of cognitive mechanisms identified by the RL model is provided in Table 1 and Appendix B.

These results also provide an interesting perspective for theorists working on models of human risky choice, a domain where substantial research effort has been devoted to identifying systematic deviations from rationality and developing heuristics and biases to account for human irrational behaviors [35, 18, 13, 14]. In contrast, the RL model highlights calculating expected values and risk aversion as the dominant forces driving the explanation and prediction of human risky choices. This finding suggests that greater attention should be paid to rational characterizations of human behavior and that there may be value in developing new theories grounded in rational principles. Recent work in this area suggests that human decisions may be explained in terms of the rational use of cognitive resources [12, 22, 41].

## 5 Control Experiments

**Data control.** To further validate the RL method, we conducted a control experiment in which the original human choice rates were replaced with synthetic choice rates generated by an expected-value maximization model. Specifically, the synthetic choice rate for option B was set to 1 if option B had a greater expected value than option A, and 0 if it had a smaller expected value. In cases where the expected values of the two options were equal, the synthetic choice rate was set to 0.5.

Using the synthetic choice rate as the reward signal for RL (i.e., replacing  $p^B$  in Equation 1 with the synthetic choice rate), we find that the RL model quickly learns to generate CoT focused on computing and comparing expected values (see Figure 6b and Appendix D for details). Although risk aversion is no longer necessary to explain the synthetic data, the model still occasionally includes references to it in its CoT. This may be due to residual cues in the prompt suggesting that the task involves human risky choice (see Appendix A.2 for details), even though the actual data had been replaced with synthetic data. Nonetheless, the RL model correctly identifies relevant cognitive mechanisms – such as rational choice theory and all-or-nothing thinking – as important for explaining the synthetic data. These results suggest that RL is capable of adapting its reasoning strategies to match the structure of the training data.

**Model control.** Additionally, we replicated the main experiment using a smaller and arguably weaker backbone LLM, Gemma-2-2B-Instruct [33] (see Appendix E for details). The same LoRA configuration was applied, resulting in approximately 41.53M trainable parameters, corresponding to 1.56% of the total parameters in the 2B model. The Gemma model was fine-tuned using SFT, Centaur-style SFT, and RL on the same training set as in the main experiment and evaluated on the same held-out test set.

We observe several noteworthy findings. First, RL applied to the Gemma model performs significantly worse than both SFT and Centaur-style SFT in reducing MSE on the test set (see Figure 10 in Appendix E). This is a pattern that contrasts with the learning curves obtained using the stronger Qwen model. Second, analysis of the CoT generated during RL training reveals that the Gemma model fails to compute and compare the expected values of the risky options, a mechanism identified as critical for explaining human behavior in the main experiment (see Appendix E). This absence of

key cognitive mechanisms in its CoT likely contributes to the weaker performance of RL on smaller models. Finally, even when RL underperforms, both SFT and Centaur-style SFT are still able to predict human behavior (albeit without explanation) at a level comparable to that of the stronger Qwen model. These suggest that RL and SFT may exhibit different generalization patterns [7, 37].

## 6 Discussion

The emergence of reasoning LLMs presents new opportunities for addressing complex problems that traditional, non-reasoning LLMs struggle to solve. This improvement is likely due to the fact that CoT reasoning enhances the expressiveness of Transformer-based models [21]. Moreover, RL post-training has been shown to effectively elicit appropriate CoTs from backbone LLMs [32, 40]. This process can be seen as analogous to learning to reason like a psychologist: given sufficient capacity, the backbone LLM implicitly encodes a range of psychological theories about human risky choice, and RL serves to surface the most relevant theoretical representations through the generation of CoT reasoning. As a result, we trained an LLM-based psychological theorist capable of verbalizing relevant cognitive mechanisms for explaining and predicting human risky choices.

**Failures of RL.** During our experiments, we also observed several failures associated with GRPO training. Most notably, applying the original GRPO algorithm [32] to the `choices13k` dataset led to mode collapse. By mode collapse, we refer to the phenomenon in which the fine-tuned LLMs converge to generating a single, repetitive reasoning chain that simply computes the expected values of both options and consistently outputs a final prediction of 50% for each option across all choice problems. Note that the `choices13k` dataset exhibits a modal human choice proportion of 50%, which may have contributed to this degeneracy.

We experimented with several strategies to prevent the model from collapsing to this default prediction. Specifically, we tested alternative reward functions, including one minus the mean squared error, negative cross-entropy loss, and the addition of diversity bonuses incentivizing diverse predictions. However, none of these modifications were effective in mitigating mode collapse in our setting.

The issue was eventually addressed by removing advantage normalization in GRPO, as recommended by [23]. That is, dividing the centered reward by the standard deviation of group rewards introduces a bias toward question-level difficulty: risky-choice problems with lower standard deviations (i.e., those that are either too easy or too difficult) disproportionately influence policy updates by receiving higher weights. By omitting this normalization step, we were able to recover the main RL results reported above.

**The elicitation hypothesis.** A prominent hypothesis about RL post-training is that it primarily increases the probability of generating correct outputs by eliciting behaviors already latent in the pretrained LLM [20, 40]. In this view, RL post-training does not teach new capabilities but instead amplifies and selects from pre-existing knowledge. Our model control results support this hypothesis: weaker LLMs—particularly those unable to elicit the expected value mechanism for risky choice—struggle to explain human behavior effectively when trained with RL. These results suggest that the success of RL highly depends on the capacity of the backbone LLM.

**Limitations and future research.** A key limitation of developing cognitive models through CoT lies in the elicitation hypothesis of RL post-training. If this hypothesis holds, RL is unlikely to generate entirely novel theories or cognitive mechanisms. For instance, imagine an LLM pretrained in a world prior to the development of Kahneman and Tversky’s prospect theory [18]. RL alone would likely not discover this theory during post-training. However, in principle, RL can draw on theoretical frameworks beyond psychology to explain psychological phenomena. For example, it may learn to apply concepts from physics or computer science to human behavior, provided such ideas are already embedded in the backbone LLM. Future research could explore how RL facilitates the integration of knowledge across traditional disciplinary boundaries to generate novel explanatory frameworks.

Our work is also constrained by computational resources, as RL is substantially more computationally intensive than SFT. Moreover, our findings suggest that RL and SFT exhibit different generalization patterns. Further research is needed to systematically investigate these differences and understand the conditions under which each method performs the best. An additional open question is when and how to effectively combine RL and SFT to produce more robust and interpretable cognitive models through the CoT of LLMs.

**Conclusion.** We introduced a method for developing interpretable cognitive models using LLMs by eliciting CoT reasoning through RL post-training, using human risky choice as a case study. Our results show that RL post-training can generate meaningful CoTs that adapt to the structure of the training data, though the effectiveness of this approach strongly depends on the capabilities of the backbone LLM. We believe this method is highly generalizable and holds promise for applications in other domains of cognitive modeling.

**Acknowledgments.** JQZ and TLG acknowledge support from the NOMIS Foundation and computing resources provided by Princeton Language and Intelligence. HX acknowledges support from the OpenAI Researcher Access Program. RCW acknowledges funding from a SCIALOG Award (#29079) from the Research Corporation for Scientific Advancement. HX and RCW also acknowledge computing support in part through research cyberinfrastructure resources and services provided by the Partnership for an Advanced Computing Environment at the Georgia Institute of Technology, USA. DA and TLG were supported by ONR MURI N00014-24-1-2748.

## References

- [1] Abdullah Almaatouq, Thomas L Griffiths, Jordan W Suchow, Mark E Whiting, James Evans, and Duncan J Watts. Beyond playing 20 questions with nature: Integrative experiment design in the social and behavioral sciences. *Behavioral and Brain Sciences*, 47:e33, 2024.
- [2] Marcel Binz, Elif Akata, Matthias Bethge, Franziska Brändle, Fred Callaway, Julian Coda-Forno, Peter Dayan, Can Demircan, Maria K Eckstein, Noémi Éltető, et al. Centaur: a foundation model of human cognition. *arXiv preprint arXiv:2410.20268*, 2024.
- [3] Marcel Binz and Eric Schulz. Turning large language models into cognitive models. *arXiv preprint arXiv:2306.03917*, 2023.
- [4] Tom Brown, Benjamin Mann, Nick Ryder, Melanie Subbiah, Jared D Kaplan, Prafulla Dhariwal, Arvind Neelakantan, Pranav Shyam, Girish Sastry, Amanda Askell, et al. Language models are few-shot learners. *Advances in Neural Information Processing Systems*, 33:1877–1901, 2020.
- [5] Jerome R Busemeyer and Adele Diederich. *Cognitive modeling*. Sage, 2010.
- [6] Pablo Samuel Castro, Nenad Tomasev, Ankit Anand, Navodita Sharma, Rishika Mohanta, Aparna Dev, Kuba Perlin, Siddhant Jain, Kyle Levin, Noémi Éltető, et al. Discovering symbolic cognitive models from human and animal behavior. *bioRxiv*, pages 2025–02, 2025.
- [7] Tianzhe Chu, Yuexiang Zhai, Jihan Yang, Shengbang Tong, Saining Xie, Dale Schuurmans, Quoc V Le, Sergey Levine, and Yi Ma. SFT memorizes, RL generalizes: A comparative study of foundation model post-training. *arXiv preprint arXiv:2501.17161*, 2025.
- [8] Michele Cohen and Jean-Yves Jaffray. Certainty effect versus probability distortion: An experimental analysis of decision making under risk. *Journal of Experimental Psychology: Human Perception and Performance*, 14(4):554, 1988.
- [9] Simon Farrell and Stephan Lewandowsky. *Computational modeling of cognition and behavior*. Cambridge University Press, 2018.
- [10] Craig R Fox and Amos Tversky. Ambiguity aversion and comparative ignorance. *The Quarterly Journal of Economics*, 110(3):585–603, 1995.
- [11] Michael C Frank and Noah D Goodman. Cognitive modeling using artificial intelligence. *OSF*, 2025.
- [12] Samuel J Gershman, Eric J Horvitz, and Joshua B Tenenbaum. Computational rationality: A converging paradigm for intelligence in brains, minds, and machines. *Science*, 349(6245):273–278, 2015.
- [13] Gerd Gigerenzer and Wolfgang Gaissmaier. Heuristic decision making. *Annual Review of Psychology*, 62(2011):451–482, 2011.
- [14] Thomas Gilovich, Dale Griffin, and Daniel Kahneman. *Heuristics and biases: The psychology of intuitive judgment*. Cambridge University Press, 2002.

- [15] Thomas L Griffiths, Nick Chater, and Joshua B Tenenbaum. *Bayesian models of cognition: reverse engineering the mind*. MIT Press, 2024.
- [16] Edward J Hu, Yelong Shen, Phillip Wallis, Zeyuan Allen-Zhu, Yuanzhi Li, Shean Wang, Lu Wang, Weizhu Chen, et al. LoRA: Low-rank adaptation of large language models. *International Conference of Learning Representations*, 1(2):3, 2022.
- [17] Liqiang Huang. A quasi-comprehensive exploration of the mechanisms of spatial working memory. *Nature Human Behaviour*, 7(5):729–739, 2023.
- [18] Daniel Kahneman and Amos Tversky. Prospect theory: An analysis of decision under risk. In *Handbook of the fundamentals of financial decision making: Part I*, pages 99–127. World Scientific, 2013.
- [19] Woosuk Kwon, Zhuohan Li, Siyuan Zhuang, Ying Sheng, Lianmin Zheng, Cody Hao Yu, Joseph E. Gonzalez, Hao Zhang, and Ion Stoica. Efficient memory management for large language model serving with pagedattention. In *Proceedings of the ACM SIGOPS 29th Symposium on Operating Systems Principles*, 2023.
- [20] Nathan Lambert. Reinforcement learning from human feedback. *arXiv preprint arXiv:2504.12501*, 2025.
- [21] Zhiyuan Li, Hong Liu, Denny Zhou, and Tengyu Ma. Chain of thought empowers transformers to solve inherently serial problems. *arXiv preprint arXiv:2402.12875*, 1, 2024.
- [22] Falk Lieder and Thomas L Griffiths. Resource-rational analysis: Understanding human cognition as the optimal use of limited computational resources. *Behavioral and Brain Sciences*, 43:e1, 2020.
- [23] Zichen Liu, Changyu Chen, Wenjun Li, Penghui Qi, Tianyu Pang, Chao Du, Wee Sun Lee, and Min Lin. Understanding R1-zero-like training: A critical perspective. *arXiv preprint arXiv:2503.20783*, 2025.
- [24] Ilya Loshchilov and Frank Hutter. Decoupled weight decay regularization. *arXiv preprint arXiv:1711.05101*, 2017.
- [25] Wei Ji Ma, Konrad Paul Kording, and Daniel Goldreich. *Bayesian models of perception and action: An introduction*. MIT Press, 2023.
- [26] Joshua C Peterson, David D Bourgin, Mayank Agrawal, Daniel Reichman, and Thomas L Griffiths. Using large-scale experiments and machine learning to discover theories of human decision-making. *Science*, 372(6547):1209–1214, 2021.
- [27] Drazen Prelec. The probability weighting function. *Econometrica*, pages 497–527, 1998.
- [28] Nils Reimers and Iryna Gurevych. Sentence-bert: Sentence embeddings using siamese bert-networks. In *Proceedings of the 2019 Conference on Empirical Methods in Natural Language Processing*. Association for Computational Linguistics, 11 2019.
- [29] Milena Rmus, Akshay K Jagadish, Marvin Mathony, Tobias Ludwig, and Eric Schulz. Towards automation of cognitive modeling using large language models. *arXiv preprint arXiv:2502.00879*, 2025.
- [30] David E Rumelhart, Geoffrey E Hinton, James L McClelland, et al. A general framework for parallel distributed processing. *Parallel distributed processing: Explorations in the microstructure of cognition*, 1(45-76):26, 1986.
- [31] John Schulman, Filip Wolski, Prafulla Dhariwal, Alec Radford, and Oleg Klimov. Proximal policy optimization algorithms. *arXiv preprint arXiv:1707.06347*, 2017.
- [32] Zhihong Shao, Peiyi Wang, Qihao Zhu, Runxin Xu, Junxiao Song, Xiao Bi, Huawei Zhang, Mingchuan Zhang, YK Li, Y Wu, et al. Deepseekmath: Pushing the limits of mathematical reasoning in open language models. *arXiv preprint arXiv:2402.03300*, 2024.

- [33] Gemma Team, Thomas Mesnard, Cassidy Hardin, Robert Dadashi, Surya Bhupatiraju, Shreya Pathak, Laurent Sifre, Morgane Rivière, Mihir Sanjay Kale, Juliette Love, et al. Gemma: Open models based on Gemini research and technology. *arXiv preprint arXiv:2403.08295*, 2024.
- [34] Amos Tversky and Daniel Kahneman. The framing of decisions and the psychology of choice. *Science*, 211(4481):453–458, 1981.
- [35] Amos Tversky and Daniel Kahneman. Advances in prospect theory: Cumulative representation of uncertainty. *Journal of Risk and Uncertainty*, 5:297–323, 1992.
- [36] Laurens Van der Maaten and Geoffrey Hinton. Visualizing data using t-SNE. *Journal of Machine Learning Research*, 9(11), 2008.
- [37] Yiping Wang, Qing Yang, Zhiyuan Zeng, Liliang Ren, Lucas Liu, Baolin Peng, Hao Cheng, Xuehai He, Kuan Wang, Jianfeng Gao, et al. Reinforcement learning for reasoning in large language models with one training example. *arXiv preprint arXiv:2504.20571*, 2025.
- [38] An Yang, Baosong Yang, Beichen Zhang, Binyuan Hui, Bo Zheng, Bowen Yu, Chengyuan Li, Dayiheng Liu, Fei Huang, Haoran Wei, et al. Qwen2. 5 technical report. *arXiv preprint arXiv:2412.15115*, 2024.
- [39] Qiying Yu, Zheng Zhang, Ruofei Zhu, Yufeng Yuan, Xiaochen Zuo, Yu Yue, Tiantian Fan, Gaohong Liu, Lingjun Liu, Xin Liu, et al. DAPO: An open-source LLM reinforcement learning system at scale. *arXiv preprint arXiv:2503.14476*, 2025.
- [40] Yang Yue, Zhiqi Chen, Rui Lu, Andrew Zhao, Zhaokai Wang, Shiji Song, and Gao Huang. Does reinforcement learning really incentivize reasoning capacity in LLMs beyond the base model? *arXiv preprint arXiv:2504.13837*, 2025.
- [41] Jian-Qiao Zhu and Thomas L Griffiths. Computation-limited Bayesian updating: A resource-rational analysis of approximate Bayesian inference. *PsyArXiv*.
- [42] Jian-Qiao Zhu, Joshua C Peterson, Benjamin Enke, and Thomas L Griffiths. Capturing the complexity of human strategic decision-making with machine learning. *arXiv preprint arXiv:2408.07865*, 2024.
- [43] Jian-Qiao Zhu, Haijiang Yan, and Thomas L Griffiths. Language models trained to do arithmetic predict human risky and intertemporal choice. *arXiv preprint arXiv:2405.19313*, 2024.

## A Prompts

### A.1 Prompts for the SFT and Centaur-style SFT models

**User:** You are a knowledgeable and insightful psychological theorist, skilled in analyzing human behavior, cognition, and decision-making. You will be shown two options, A and B. Your task is to estimate the proportion of people who will choose each option. Please only provide your final estimates in JSON format, ensuring that: “option\_A” represents the percentage of people choosing Option A; “option\_B” represents the percentage of people choosing Option B; The values must be numbers between 0 and 100 (inclusive); The sum of “option\_A” and “option\_B” must equal 100.

### A.2 Prompts for the RL model

**User:** You are a knowledgeable and insightful psychological theorist, skilled in analyzing human behavior, cognition, and decision-making. You will be shown two options, A and B. Your task is to estimate the proportion of people who will choose each option. First, explain your reasoning step by step. Then, provide your final estimates in JSON format, ensuring that: “option\_A” represents the percentage of people choosing Option A; “option\_B” represents the percentage of people choosing Option B; The values must be numbers between 0 and 100 (inclusive); The sum of “option\_A” and “option\_B” must equal 100.

### A.3 Example prompts for risky options

Risky choices from the `choices13k` dataset are described in natural language using the following format:

Option A offers (1) a 50.0% chance to win \$2.0; (2) a 50.0% chance to win \$0.0.

Option B offers a 100.0% chance to win \$1.0.

## B Cognitive mechanisms identified by Qwen-2.5-7B-Instruct

Based on the CoT reasoning generated by the RL models, we identified a set of cognitive mechanisms that the model appeared to find useful for predicting human risky choices. To assist with summarization, we used GPT-4.1 with the following prompt (the temperature for GPT-4.1 was fixed at 0):

**User:** Read the following thought atom and return a JSON list of standard psychological effects or cognitive biases that are present. Use only the most relevant terms from established psychological concepts (e.g., “Expected Value”, “Loss Aversion”, “Risk Aversion”, etc.). Return only a JSON list like [“Effect1”, “Effect2”, ...]. No explanation or extra text.

Cognitive mechanisms that appeared in at least 10 risky-choice problems are summarized in Table 1. Other mechanisms identified in the CoT reasoning are described below: *Social Proof, Reference Point, Reference Dependence, Behavioral Biases, Rational Choice Theory, Majority Effect, Gambler’s Fallacy, Anchoring Effect, Risk Neutrality, Heuristic, Present Bias, Perceived Utility, Risk Premium, Representativeness Heuristic, Regret Aversion, Perceived Value, Heuristic Processing, Range Effect, Assumption Bias, Attractiveness Effect, Risk Assessment, Underweighting of Large Probabilities, Simplicity Preference, Perceived Risk, Simplicity Bias, Assumption of Uniformity, Diminishing Sensitivity, Variance Aversion, Diversification Bias, Variance Preference, Cognitive Biases, Mental Accounting, Endowment Effect, Neglect of Expected Value, Heuristic Bias, Overestimation of Small Probabilities, Heuristic Simplification, Sure-Thing Principle, Frequency Illusion, Psychological Biases, Pessimism Bias, Immediate Gratification, Preference for Variety, Ambiguity Effect, Overweighting of Gains, Immediate Reward Bias, Diversification Effect, Overestimation of Rare Events, Contrast Effect, Regret Theory, Multiple Gains Effect, Equally Likely Heuristic, Approximation Bias, Overweighting Small Probabilities, Positivity Effect, Salience of Losses, Affect Heuristic, Windfall Effect, Underweighting of Losses, Magnitude Effect, Majority Influence, Frequency Effect, Nonlinear Utility, Risk-Reward Tradeoff, Sure Thing Effect, Heuristic Biases, Overconfidence Effect, Preference for Simplicity, Law of Small Numbers, Attractiveness Heuristic, Denomination Effect, Cognitive Ease, Estimation Bias, Value Perception, Allais Paradox, Probability Perception, Utility of Money, Psychophysical Numbing, Hope Effect, Assumption of Symmetry, Simplicity Effect, Salience, Decision Heuristics, Probability Matching, Weber-Fechner Law, Satiation, Overconfidence Bias, Assumption of Probability Distribution, Assumption Heuristic, Small Wins Effect, Reward Seeking, Intuition, Neglect of Probability Weighting, Lottery Effect, Time Preference, Range Seeking, Impact Bias, Positive Outcome Bias, Reference Points, Fairness Bias, Risk Seeking in Losses, Loss Underestimation, Heuristic Substitution, Behavioral Economics, Temporal Discounting, Risk-Reward Ratio, Lump Sum Effect, Overestimation, Gambling Fallacy, Variety Seeking, Framing, Variability Effect, Anchoring Bias, Risk-Seeking, Heuristic Reasoning, Conservatism Bias, Delay Discounting, Undervaluation of Large Losses, Overweighting of Large Gains, Reward Sensitivity, Minimization of Differences, Reference Point Effect, Uncertainty Aversion, Simplification, Underweighting of Small Probabilities, Immediate Reward Preference, Overestimation Effect, Motivational Salience, Overweighting of Outcomes, All-or-Nothing Thinking, Simplification Bias, Equal Probability Bias, Segregation of Gains, Choice Overload, Social Norms, Majority Illusion, Near Miss Effect, Psychological Value of Money, Frequency Bias, Normalization, Emotional Valence, Risk-seeking Behavior.*

## C Additional analyses of CoT

### C.1 Human evaluation of CoT

To obtain a preliminary human evaluation of CoT reasoning quality, we conducted the following experiment.

Table 1: Frequency of cognitive mechanisms identified in the CoT reasoning generated by the RL model (final checkpoint). Only mechanisms that appeared in at least 10 risky-choice problems are reported.

Cognitive mechanism	Count
Expected value	6495
Risk aversion	5210
Loss aversion	1676
Certainty effect	1453
Risk seeking	710
Probability weighting	470
Framing effect	278
Prospect theory	113
Ambiguity aversion	99
Risk perception	76
Overweighting of small probabilities	64
Risk tolerance	64
Heuristics	51
Attraction effect	50
Assumption of equiprobability	49
Equiprobability bias	41
Diminishing marginal utility	38
Optimism bias	37
Risk preference	34
Possibility effect	30
Utility theory	23
Expected utility theory	19
Availability heuristics	19
Anchoring	18
Variance effect	15
Bandwagon effect	14
Salience bias	13
Diversification	12
Probability overestimation	12
Assumption of equal probability	12
Complexity aversion	11
Expected utility	10
Expected value neglect	10

**Participants.** We recruited 20 participants via a social media post targeting local universities, inviting volunteers to evaluate completions generated by LLMs. The sample included 12 graduate students, 3 postdoctoral researchers, 3 faculty members, and 2 undergraduate students. Participants represented a range of academic disciplines: 10 from Psychology or Cognitive Science, 7 from Computer Science or Artificial Intelligence, and 3 from Business or Economics. On average, participants reported a self-assessed knowledge of human risky decision-making of 3.5 out of 5. Participants did not receive any monetary payment, and the study lasted up to 30 minutes. All experimental sessions were conducted in May 2025. Informed consent was obtained from all participants (Princeton University IRB number 10859: “Computational Cognitive Science”)

**Procedures.** Each participant completed 10 evaluation trials. On each trial, a risky choice problem was randomly sampled from the held-out test set. The corresponding CoT completions generated by the backbone and RL models were presented side by side beneath the problem statement (see Figure 7 for an example). To ensure that evaluations focused on reasoning quality rather than predictive accuracy, we removed the final choice predictions from the completions. Participants were instructed to select which CoT they found more reasonable by making a binary choice. After each choice, they also reported their confidence using a slider ranging from 0 (least confident) to 100 (most confident). To prevent bias, the two completions were anonymized as Model A and Model B, and their left-right order was randomized across trials.

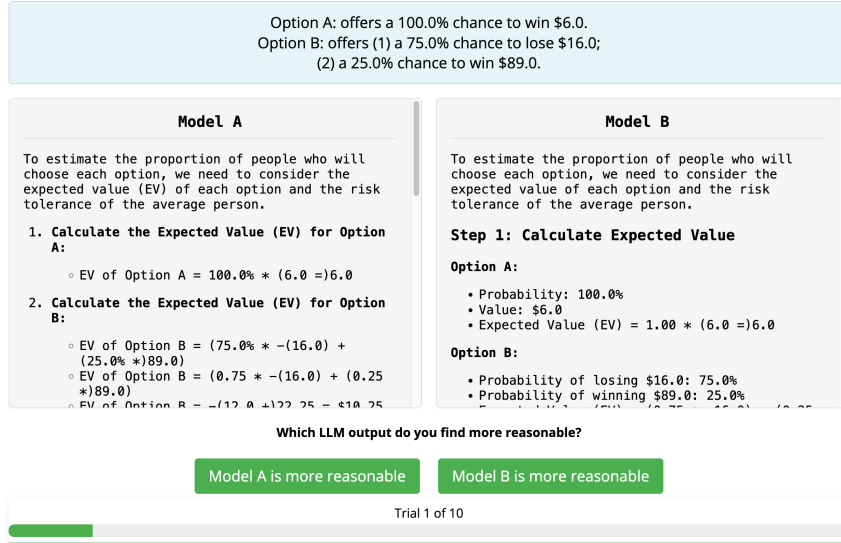


Figure 7: Screenshot of a representative trial from the human evaluation experiment. Participants were shown a risky choice problem followed by two anonymized CoT completions (Model A and Model B) and asked to select the more reasonable explanation.

**Results.** On average, CoTs generated by the RL model were selected as more reasonable in 61.5% of trials ( $SE = 5.2\%$ ) above the chance level of 50% at 0.05 significance level ( $t(19) = 2.19, p < .05$ ). This suggests that participants found the reasoning produced by the RL model to be more persuasive or coherent than that of the backbone model. While this represents a useful initial step in soliciting expert opinions from researchers in relevant fields, scaling human evaluations to the whole dataset remains a significant challenge.

## C.2 Using GPT-4.1 to judge CoT

Due to the large volume of CoTs generated across multiple model checkpoints and risky choice problems, conducting comprehensive human evaluations is constrained by time and labor demands. To address this limitation, we piloted an alternative approach using GPT-4.1 to simulate expert evaluations. Specifically, GPT-4.1 was instructed to role-play as an expert in judgment and decision-making and provide quality ratings of the CoTs. The temperature for GPT-4.1 was fixed at 0. The model was prompted with the following instructions:

**System:** You are an expert in judgment and decision-making.

**User:** As an expert in judgment and decision-making, please evaluate the reasoning and prediction of the following question. Provide a single integer score from 0 to 100 based on the quality of the completion.

As shown in Figure 8, GPT-4.1’s ratings of the RL model’s completions show a modest initial increase, though the magnitude of change is relatively small given the full rating scale of 0 to 100. The scores then stabilize for several training steps before exhibiting a slight decline toward the end. This pattern suggests that the quality of the CoT reasoning largely plateaued after the first epoch of RL training.

## C.3 Swapping CoT between backbone and RL models

To examine the potential causal relationship between CoT reasoning and final predictions of human choice proportions, we conducted the following analysis. First, we evaluated both the original backbone LLM (i.e., Qwen-2.5-7B-Instruct, or checkpoint 0) and its RL post-trained version (i.e., the final RL checkpoint) on the test set, recording their generated CoTs and final predictions (see the first row of Table 2). Next, we removed the final JSON prediction from each model’s completion and

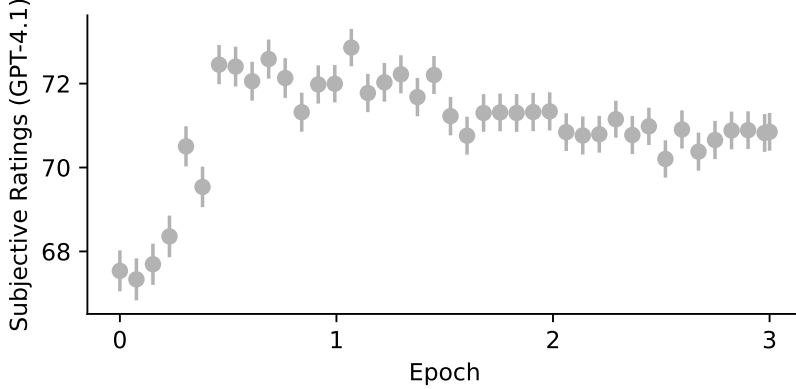


Figure 8: GPT-4.1 was prompted to act as an expert evaluator, rating the RL model’s completions for risky-choice problems in the test set. Error bars represent  $\pm 1$  standard error across choice problems.

performed a CoT-swapping procedure: the backbone LLM was prompted with the RL model’s CoT and asked to continue the generation, while the RL model was prompted with the backbone LLM’s CoT and similarly asked to produce a final prediction (see the second row of Table 2).

We find that using the RL model’s CoT significantly reduces the backbone model’s prediction error, as measured by MSE ( $t(2596) = -18.11, p < .01$ ). Conversely, using the backbone model’s CoT significantly increases the RL model’s prediction error ( $t(2597) = 20.65, p < .01$ ). These results suggest that the RL model generates higher-quality CoTs that contribute more effectively to accurate final predictions than those produced by the backbone model.

Table 2: Prediction errors for the backbone LLM and its RL post-trained counterpart. Values represent mean squared error on the test set, with standard errors in parentheses. Original CoT indicates that the model used its own CoT reasoning for prediction, whereas Swapped CoT refers to predictions made using the CoT generated by the other model.

	Qwen-2.5-7B-Instruct (backbone)	Qwen-2.5-7B-GRPO-c13k (RL)
Original CoT	.0694 (.0025)	.0148 (.0006)
Swapped CoT	.0212 (.0008)	.0695 (.0025)

## D Data control experiment

### D.1 Learning curves

In the data control experiment, we retained the same backbone LLM, Qwen-2.5-7B-Instruct, but replaced the human data with synthetically generated data from an expected-value maximization model. We then performed RL post-training on this synthetic dataset using the same set of hyperparameters as in the main experiment. The RL learning curve shows a gradual improvement in model performance over training steps (see Figure 9).

### D.2 Cognitive mechanisms identified by Qwen-2.5-7B-Instruct during the data control experiment

We replicated the CoT analysis presented in Appendix B for the RL model trained on the synthetic choice dataset in the control experiment. The evolution of the top eight cognitive mechanisms identified in the model’s CoT reasoning across training epochs is shown in Figure 6b. Given that the synthetic choice rates were generated by an expected-value maximizer model, the expected value computation emerges as the dominant mechanism in the CoT.

The full list of cognitive mechanisms, ordered by frequency of use, is presented below: *Expected Value, Risk Aversion, Rational Choice Theory, All-or-Nothing Thinking, Black-and-White Thinking,*

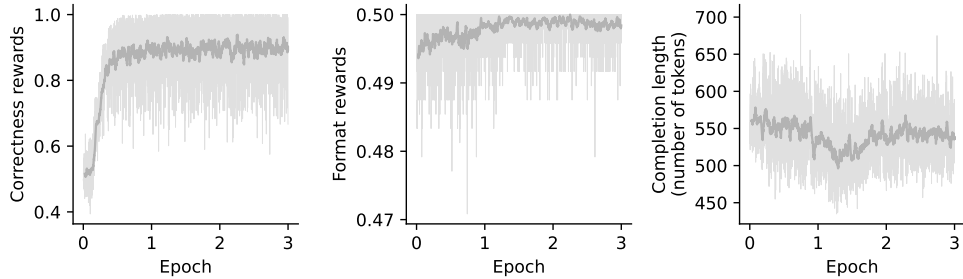


**Figure 9: Data control experiment.** Learning curves for the RL model. Backbone LLM is Qwen-2.5-7B-Instruct. (*Left*) Correctness reward, defined as one minus the absolute difference between model predictions and human choice proportions. (*Middle*) Format reward, based on the structure and position of the model’s JSON output. (*Right*) Completion length, measured by the number of generated tokens.

*Certainty Effect, Herd Behavior, Bandwagon Effect, Consensus Bias, Expected Utility Theory, Zero-Sum Bias, Overconfidence Effect, Loss Aversion, Risk Seeking, Probability Neglect, Majority Influence, False Consensus Effect, Dominance Heuristic, Indifference, Overconfidence Bias, Overweighting of Small Probabilities, Indifference Principle, Binary Bias, Social Proof, Majority Effect, Equiprobability Bias, Contrast Effect, Optimism Bias, Risk Neutrality, Indifference Point, Expected Utility, Ambiguity Aversion, Equity Heuristic, Normative Decision Theory*

## E Model control experiment

### E.1 Learning curves

In the model control experiment, we replaced the original Qwen-2.5-7B-Instruct model with the smaller Gemma-2-2B-Instruct model, while keeping the human risky choice data as the target for prediction. We find that SFT and Centaur-style SFT achieve comparable levels of predictive accuracy (see Figure 10). At the final checkpoint, the MSE on the test set is  $M = 0.0162$ ,  $SE = 0.0006$  for SFT and  $M = 0.0163$ ,  $SE = 0.0007$  for Centaur-style SFT, with no statistically significant difference between them ( $t(2924) = -0.13$ ,  $p = 0.90$ ). In contrast, RL yields significantly higher MSE at its final checkpoint ( $M = 0.0526$ ,  $SE = 0.0016$ ), indicating poorer predictive performance.

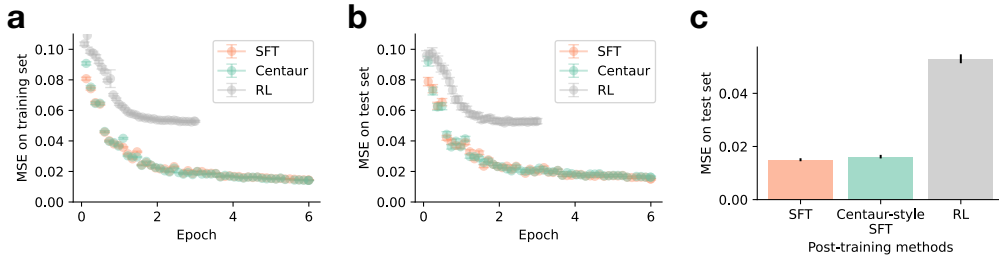


**Figure 10: Model control experiment.** Learning curves on the (a) training and (b) test sets. Backbone LLM is Gemma-2-2B-Instruct. The horizontal axes indicate training epochs, while the vertical axes represent mean squared error (MSE) evaluated on the corresponding dataset. The three post-training strategies compared are supervised fine-tuning (SFT, red), Centaur-style SFT (green), and reinforcement learning using Group Relative Policy Optimization (RL, grey). (c) MSE on the test set at the final checkpoint of each post-training method. Error bars represent  $\pm 1$  standard error across risky-choice problems.

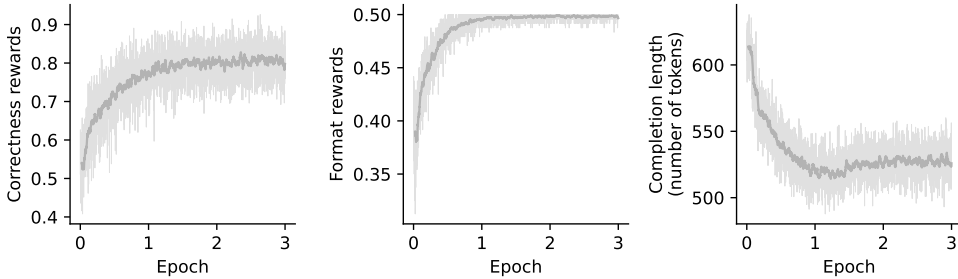


**Figure 11: Model control experiment.** Learning curves for the RL model. Backbone LLM is Gemma-2-2B-Instruct. (*Left*) Correctness reward, defined as one minus the absolute difference between model predictions and human choice proportions. (*Middle*) Format reward, based on the structure and position of the model’s JSON output. (*Right*) Completion length, measured by the number of generated tokens.

## E.2 Cognitive mechanisms identified by Gemma-2-2B-Instruct

As before, we replicated the CoT analysis (see Appendix B) for the RL model trained using the Gemma-2-2B-Instruct backbone. This model performs poorly in predicting human choices compared to both SFT-based methods applied to the same LLM and RL applied to the stronger Qwen model. The distribution of identified cognitive mechanisms in the CoT provides insight into this performance gap (see Figure 12). Notably, the CoT lacks arguably the most critical component: expected value calculation and comparison. The absence or infrequent usage of this key cognitive mechanism likely contributes to the RL model’s failure to accurately capture human risky choice.

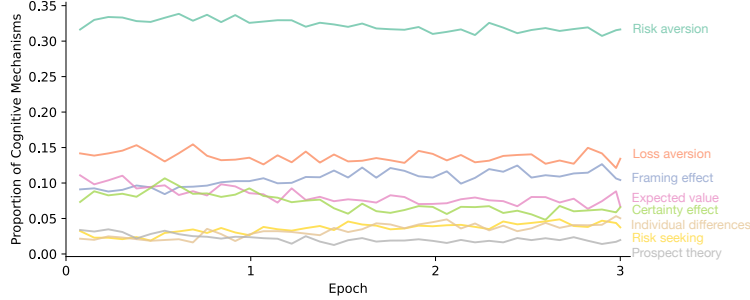


**Figure 12: Model control experiment.** Proportions of cognitive mechanisms identified in the RL models’ thoughts across training epochs. Backbone LLM is Gemma-2-2B-Instruct. The top 8 most frequently used mechanisms are displayed.

Additional identified mechanisms are listed below in order of frequency: *Ambiguity Aversion, Risk Tolerance, Probability Weighting, Anchoring, Subjective Probability, Anchoring Bias, Probability Neglect, Anchoring Effect, Status Quo Bias, Mental Accounting, Affect Heuristic, Uncertainty Aversion, Immediate Gratification, Social Proof, Endowment Effect, Optimism Bias, Confirmation Bias, Present Bias, Heuristics, Social Influence, Availability Heuristic, Attraction Effect, Context Effect, Opportunity Cost, Possibility Effect, Regret Aversion, Overconfidence Effect, Gambler’s Fallacy, Hedonic Adaptation, Personality Traits, Lottery Effect, Reward Sensitivity, Overweighting of Small Probabilities, Choice Overload, Emotional Reasoning, Impulsivity, Comparative Judgment, Groupthink, Reward Seeking, Cognitive Bias, Cognitive Dissonance, Stress Influence on Decision Making, Cognitive Complexity, Desire for Gain, Pessimism Bias, Relative Value, Cognitive Biases, Information Overload, Mood Congruent Bias, Expected Utility Theory, Immediate Reward Bias, Probability Perception, Subjective Value, Illusion of Control, Perceived Probability, Desirability Bias, Heuristic, Cognitive Load, Bounded Rationality, Sunk Cost Fallacy, Ambiguity Effect, Positivity Bias, Comparative Evaluation, Cognitive Appraisal, Perceived Value, Normative Social Influence, Expected Value Neglect, Herd Behavior, Context Dependence, Incentive Salience, Risk Perception,*

*Intuition, Subjective Utility, Salience Bias, Subjectivity, Neglect of Probability, Personal Experience Effect, Magnitude Effect, Motivation, Overestimation of Small Probabilities, Hope, Hot-Hand Fallacy, Information Asymmetry, Probability Overestimation, Value of Money, Mental Fatigue, Complexity Aversion, Uncertainty Effect, Reference Dependence, Time Pressure, Perceived Predictability, Fear of Missing Out.*

## F Implementation details

**7B models.** RL training was conducted over 3 epochs using the training set, distributed across  $4 \times$ H100 GPUs for a total runtime of 80 hours. For SFT and Centaur-style SFT trainings, each model was trained for 6 epochs on the training set, using a single A100 GPU with an approximate runtime of 5 hours per training session.

Inference across all checkpoints on the complete `choices13k` dataset took approximately 5 hours on a single A100 GPU for the SFT and Centaur-style SFT models using vLLM [19], whereas the RL models required roughly 30 hours under the same conditions.

**2B models.** RL training was conducted over 3 epochs using the training set, distributed across  $4 \times$ H100 GPUs for a total runtime of 40 hours. For SFT and Centaur-style SFT trainings, each model was trained for 6 epochs on the training set, using a single A100 GPU with an approximate runtime of 3 hours per training session.

Inference across all checkpoints on the complete `choices13k` dataset took approximately 3 hours on a single A100 GPU for the SFT and Centaur-style SFT models using vLLM [19], whereas the RL models required roughly 20 hours under the same conditions.

**Preliminary or failed experiments.** We also conducted several pilot studies and unsuccessful RL runs, which together accounted for approximately 2,000 H100 GPU hours.